Proceedings of the ASME 2010 3rd Joint US-European Fluids Engineering Summer Meeting and 8th International Conference on Nanochannels, Microchannels, and Minichannels
FEDSM-ICNMM2010
August 1-5, 2010, Montreal, Canada

FEDSM-ICNMM2010-30731

EFFECT OF WALL MOVEMENT ON A JET DEPOSITING ON A MOVING WALL AT MODERATE REYNOLDS NUMBER

Md.Yahia Hussain and Roger E. Khayat
Department of Mechanical and Materials Engineering,
The University of Western Ontario
London, Ontario, Canada

ABSTRACT

The steady flow of a moderately inertial jet depositing on a moving wall, is examined theoretically near channel exit. The free surface jet emerges from a channel and adheres to a wall, which may move in the same or opposite direction to the acting channel pressure gradient. The problem is solved using the method of matched asymptotic expansions. The small parameter involved in the expansions is the inverse Reynolds number. The flow field is obtained as a composite expansion by matching the flow in the boundary layer regions near the free surface, with the flow in the core region. The influence of inertia and wall velocity on the shape of the free surface, the velocity and stress is emphasized. It is found that the viscous relaxation length is essentially uninfluenced by the velocity of a forward moving wall. In contrast, it diminishes rapidly with the velocity of a backward moving wall.

1. INTRODUCTION

The interplay between driving pressure and wall movement is examined in this study for the two-dimensional steady jet of an incompressible fluid near channel exit. The flow configuration corresponds, generically, to a pressure driven jet inside a channel, flowing or depositing onto a moving wall as it emerges out of the channel (see figure 1). The flow near the channel exit is closely examined, and the influence of inertia and wall velocity is emphasized. Inertia is assumed to remain relatively important, allowing the asymptotic development of the flow field in terms of the inverse Reynolds number. The jet is assumed to be subject to a constant pressure gradient far upstream, and the wall may move in the forward direction, adding to the action of driving pressure, or in the backward direction, opposing the driving pressure. The driving pressure is assumed to be dominant. Although the moving wall jet problem has its own challenges, it presents common fundamental characteristics with other laminar free surface jet flows which have been studied in the past.

When a free surface viscous jet emerges from a tube or a channel, an abrupt change in stress occurs at the exit. This stress singularity constitutes the major difficulty in any theoretical analysis. In particular, if a computational approach is adopted, the incorporation of the singularity point and its immediate vicinity is unavoidable since the entire flow domain must be considered (discretized). The singularity region, which is crucial to the rest of the flow domain, is difficult to handle numerically if a satisfactory level of accuracy is sought. In contrast, the asymptotic approach lends itself efficiently as a viable alternative. Asymptotic analyses tend to circumvent the singularity by identifying two distinct flow regions: a boundary layer region near the free surface, extending but not including the singular point, and a core region where the flow remains close to fully developed. The inclusion of the singularity is not essential in this case given the similarity character of the flow in the boundary layer region. Perhaps more importantly, asymptotics tend to provide deeper insight on the flow structure near the singularity. The analysis is similar to entry flows

where two distinct regions can be identified, an inviscid region and a developing boundary layer that emanates from the entrance point. At large Reynolds number, the upstream diffusion of vorticity is small, and the distortion of the original parallel streamlines is also small. The vorticity generated at the leading edge where the stress singularity occurs diffuses laterally and is convected downstream, eventually contaminating the entire flow field. Velocity changes in the inviscid core occur primarily through conservation of mass. An analogous situation occurs for the moving wall jet at large Reynolds number. The entrance length corresponds to a stress relaxation length, and the inviscid core is replaced with a viscous core in which elongation is small as a result of small axial velocity and stress gradients. Velocity gradients in this region occur primarily because of jet contraction (or expansion depending on the Reynolds number) through conservation of mass. At the exit of the channel, the shear stress drops discontinuously to zero. The effect of this drop diffuses toward the moving wall of the jet both inside (upstream) and outside (downstream) the channel. However, the diffusion is much more significant outside the channel, and is convected downstream, eventually reaching the moving wall. The original Poiseuille-Couette flow gradually acquires a boundary layer character. For a stationary wall, Watson's [1] similarity solution applies far downstream where the flow is entirely of the boundary layer type. The viscous relaxation length depends on both the driving pressure gradient and wall velocity.

Although moving wall jet flow is of fundamental importance, it is also of significant practical relevance. In particular, wall jet flow has been mainly examined in the context of the coating process, where inertia is usually neglected but is not necessarily negligible; see, for instance, the reviews of Ruschak [2] and Weinstein and Ruschak [3]. Although various coating flow configurations exist in practice, slot coating is probably of closest relevance to the current problem (see, among others, Carvalho and Kheshgi [4], Pasquali and Scriven [5], Lee *et al.* [6], Romero *et al.* [7]). Other similar coating configurations involving wall movement but with different boundary conditions are worth noting here, namely, blade coating (Ross *et al.*[8]), dip coating (Ro and Homsy [9]), and planar injection flow (Lee *et al.*).

2. GOVERNING EQUATIONS AND BOUNDARY CONDITIONS

Consider the two-dimensional flow of an incompressible fluid of density ρ and viscosity μ, emerging from a channel of width D, and depositing on a wall moving at velocity C. The flow configuration is schematically depicted in figure 1 in the (X, Z) plane. The X axis is taken along the stationary wall and the Z axis is chosen in the transverse direction across the channel. The channel exit coincides with X = 0. The flow is induced by the simultaneous action of a pressure gradient, dP/dX, inside the channel and the translation of the upper wall. The stream function of the basic Poiseuille-Couette flow is obtained from

$$\Psi = \frac{1}{2\mu}\frac{dP}{dX}\left(\frac{Z^3}{3} - D\frac{Z^2}{2}\right) + \frac{C}{2D}Z^2 = -\frac{6V}{D^2}\left(\frac{Z^3}{3} - D\frac{Z^2}{2}\right) + \frac{C}{2D}Z^2 \tag{2.1}$$

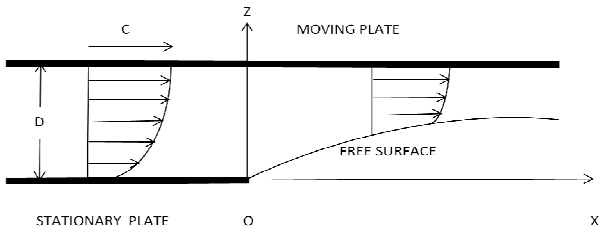

FIGURE 1. SCHEMATIC ILLUSTRATION OF THE PLANAR JET FLOW. THE JET IS PRESSURE DRIVEN OUT OF THE CHANNEL AND IS ENTRAINED BY THE TRANSLATING WALL.

where $V = -\frac{1}{12\mu}\frac{dP}{dX}D^2$ is the mean velocity due to the pressure gradient inside the channel. Note that $\frac{C}{2}$ is the mean velocity due to wall translation. In this case, *V* is assumed to be always positive and will be used as the velocity scale. In other words, the pressure gradient is assumed to be always present and negative. *C* can be positive or negative (with $C/2 > -V$), allowing for forward or backward wall movement, respectively. Non-dimensional variables are introduced by measuring lengths with respect to *D*, stream function with respect to *VD*, and pressure with respect to ρV^2. In this case, two dimensionless groups emerge in the problem, namely, the Reynolds number, Re, and the ration, *c*, of the mean Couette and mean Poiseuille velocities. Thus,

$$\mathrm{Re} = \frac{DV}{\nu}, \qquad c = \frac{C}{2V} \tag{2.2}$$

where ν is the kinematic viscosity. Now, (2.1) will turn out to be the leading order solution in the outer region, and is conveniently introduced here as

$$\psi_0 = (3+c)z^2 - 2z^3 \tag{2.3}$$

Accordingly, the flow is assumed to be solely pressure driven if c = 0, and solely induced by forward wall translation if $c \to \infty$. Also, when the mean velocity of a backward moving wall is equal to the pressure gradient inside the channel, then *c* = - 1. In this study, Re is assumed to be moderately large and *c* = O(1).

The non-dimensional conservation of momentum equation for the laminar steady flow takes the following form

$$\psi_z\psi_{xz}-\psi_x\psi_{zz}=-p_x+\frac{1}{\mathrm{Re}}\left(\psi_{xxz}+\psi_{zzz}\right) \tag{2.4a}$$

$$-\psi_z\psi_{xx}+\psi_x\psi_{xz}=-p_z-\frac{1}{\mathrm{Re}}\left(\psi_{xxx}+\psi_{xzz}\right) \tag{2.4b}$$

For x > 0, the kinematic and dynamic boundary conditions at the free surface, $z=\zeta(x)$, are

$$\psi=0 \tag{2.5a}$$

$$p+\frac{1}{\mathrm{Re}}\left[2\psi_{xz}+\zeta'\left(\psi_{zz}-\psi_{xx}\right)\right]=0 \tag{2.5b}$$

$$p\zeta'-\frac{1}{\mathrm{Re}}\left(2\psi_{xz}\zeta'-\psi_{zz}+\psi_{xx}\right)=0 \tag{2.5c}$$

A prime denotes total differentiation. Inside the channel (x < 0), the following conditions must be satisfied, namely,

$$\psi_z=2c\ ,\quad \psi_x=0 \qquad \text{at} \qquad z=1 \tag{2.6a}$$

$$\psi_z=0 \qquad \text{at} \qquad z=0 \tag{2.6b}$$

$$\psi\to(3+c)z^2-2z^3 \qquad \text{as} \qquad x\to-\infty \tag{2.6c}$$

When the fluid exits the channel, the vanishing of wall shear stress at the channel exit causes a boundary layer to develop adjacent to the free surface, which will be called the *inner layer*. This thin inner layer and the jet contraction (or expansion) affect the core of the jet, with this *core layer* remaining predominantly of inviscid rotational character.

The current study focuses on the flow outside the channel where the similarity solution in the inner layer is matched onto the core solution. This latter in turn is matched onto the solution in the core region inside the channel at the channel exit. It is important to observe that no matching is required for the similarity solution at x = 0, and the flow singularity at the origin is entirely avoided in the solution process. This constitutes a major advantage of the current formulation compared to alternative solution methods.

3. THE FLOW IN THE INNER LAYER CLOSE TO THE FREE SURFACE

To examine the boundary layer structure near the free surface, let $y=z-\zeta(x)$. In this case, the scaling in the transverse direction is changed by writing $y = \varepsilon\eta$, where $\varepsilon = \mathrm{Re}^{-\alpha}$ is the small parameter in the problem and α is to be determined. Anticipating that the height ζ of the free surface is of the same order of magnitude as the boundary layer thickness, one can write $\zeta(x) = \varepsilon h(x)$, and henceforth work with h. It is not necessary to assume that $h(x) = O(1)$ as $\varepsilon \to 0$; examination of (3.7) below shows that the inner expansion developed in this section holds provided only that $h = o(\varepsilon^{-1})$, i.e. ζ tends to 0 with ε. In the matching process, in section 5, it will be shown that h = O(1). Following Tillett [10], the following change of coordinates is introduced, namely,

$$x=\xi, \qquad z=\varepsilon(\eta+h) \tag{3.1}$$

The aim is to find a solution of the transformed equations of (2.4) in the form of an "inner expansion" in ε. In order to match this to the outer Poiseuille-Couette flow, it is necessary to have $\psi \sim y^2$ as $\eta \to \infty$ in the inner region, to lowest order in ε. Therefore, ψ must be of order ε^2. Similarly to jet flow (Tillett 1968), the value of α is determined by requiring that the convective and viscous terms balance, leading to α = 1/3. Considering the fact that u in the inner region must match the velocity in the outer region: $u\to 2(3+c)z-6z^2$, it is inferred that u must be of order ε inside the inner region. The order of w can be found using the continuity to be of order ε^2. The inner expansion for ψ begins with a term in ε^2. This is assumed, until there is evidence to the contrary. Thus, the expansion proceeds in powers of ε so that

$$\psi(\xi,\eta)=\varepsilon^2\Psi_2(\xi,\eta)+\varepsilon^3\Psi_3(\xi,\eta)+\cdots \tag{3.2}$$

Similarly, h is expanded as

$$h(\xi)=\varepsilon^{-1}\zeta(\xi)=h_0(\xi)+\varepsilon h_1(\xi)+\cdots \tag{3.3}$$

From the conservation of momentum equation, it is concluded that p is of order ε^4. Thus,

$$p(\xi,\eta)=\varepsilon^4P_4(\xi,\eta)+\varepsilon^5P_5(\xi,\eta)+\cdots \tag{3.4}$$

The velocity components are expanded as

$$u(\xi,\eta)=\varepsilon U_1(\xi,\eta)+\varepsilon^2U_2(\xi,\eta)+\cdots \tag{3.5}$$

$$w(\xi,\eta)=\varepsilon^2W_2(\xi,\eta)+\varepsilon^3W_3(\xi,\eta)+\cdots \tag{3.6}$$

In this case, $U_1 = \Psi_{2\eta}$, $U_2 = \Psi_{3\eta}$ and $W_2 = -\Psi_{2\xi} + h'_0\Psi_{2\eta}$, etc.

To leading order, the problem is similar to the case of the free jet (Tillett 1968) with different boundary conditions. A similarity solution can be carried out for Ψ_2; which is written here as

$$\Psi_2(\xi,\eta) = \xi^{2/3} f_2(\theta) \tag{3.7}$$

where $\theta = \eta\xi^{-1/3}$ is the similarity variable. The equation for $f_2(\theta)$ is given by

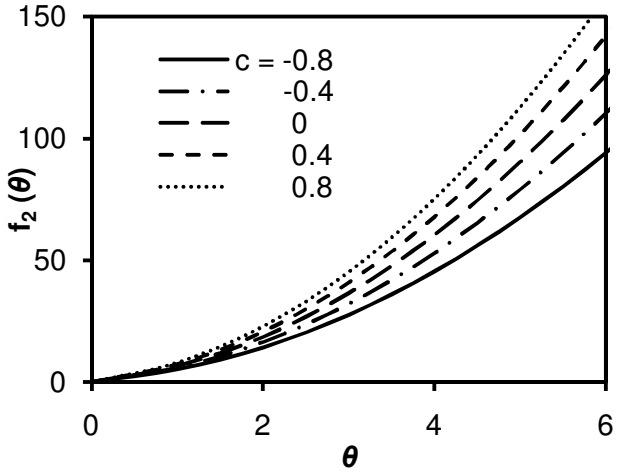

FIGURE 2. VARIATION OF THE SIMILARITY FUNCTION f_2 WITH θ FOR c ∈ [- 0.8, 0.8].

$$3f_2''' + 2f_2 f_2'' - f_2'^2 = 0 \tag{3.8}$$

subject to the following boundary conditions:

$$f_2(0) = f_2''(0) = 0 \tag{3.9a}$$

$$f_2(\theta) \sim (3+c)\theta^2 \quad \text{as} \quad \theta \to \infty \tag{3.9b}$$

Condition (3.9b) is obtained from matching, which will be discussed in section 6. An equation similar to (3.8) was investigated by Goldstein [11] and revisited by Tillett (1968). For large θ, an asymptotic solution is possible to obtain subject to condition (3.9b) following similar arguments, leading to

$$f_2(\theta \to \infty) = (3+c)(\theta + c_1)^2 + O\left[\exp\left(-\frac{2}{9}(3+c)\theta^3\right)\right] \tag{3.10}$$

where $c_1(c)$ is a c dependent constant determined from numerical integration which is determined upon matching the numerical solution and its asymptotic counterpart (3.10).

Figure 2 displays the dependence of f_2 on θ for different c values. The figure suggests that f_2 increases essentially linearly with c, pointing to a strengthening of the flow with wall velocity, which is also reflected by the increase in the slope f_2'. Interestingly, c_1 appears to be essentially independent of wall velocity and is approximately equal to 0.5. This, in turn, has an interesting consequence on the influence of wall movement on the film. As will be observed in section 5, in contrast to the velocity at the free surface, the film height is insensitive to wall movement near the channel exit.

To the next order in ε, a linear equation is obtained for Ψ_3, with variable coefficients, admitting a similarity solution of the form (Tillett 1968)

$$\Psi_3(\xi,\eta) = \xi f_3(\theta) \tag{3.11}$$

The equation for f_3 is given by

$$3f_3''' + 2f_2 f_3'' - 3f_2' f_3' + 3f_2'' f_3 = 0 \tag{3.12}$$

subject to the following boundary conditions:

$$f_3(0) = f_3''(0) = 0 \tag{3.13a}$$

The third boundary condition is obtained from matching:

$$f_3(\theta) \sim -2\theta^3 \quad as \quad \theta \to \infty \tag{3.13b}$$

An asymptotic solution similar to but more complicated than the case of free jet flow (Tillett 1968) is possible. Thus,

$$f_3(\theta \to \infty) = -2\left[(\theta + c_1)^3 - \frac{3}{3+c}\right] + c_2(\theta + c_1) + O\left[\exp\left(-\frac{2}{9}\frac{(3+c)^2}{c+1}\theta^3\right)\right] \tag{3.14}$$

The numerical integration of equation (3.12) gives the value $c_2(c)$. Figure 3 shows the f_3 profiles for different c values. In this case, f_3 and f_3' are both negative for any c value, pointing to a higher order weakening effect of wall movement on the flow near the free surface. This is seen upon taking the velocity to third order namely

$$u(x,\theta) = \varepsilon x^{1/3} f_2'(\theta) + \varepsilon^2 x^{2/3} f_3'(\theta) \tag{3.15}$$

Expression (3.15) gives the dependence of the velocity at the free surface on the velocity of the wall. The free surface velocity diminishes upon adding the higher order term, and approximately depends on c following

$$u(x, z=\zeta) = (1.2c + 5.3)\varepsilon x^{1/3} - (0.34c^2 - 1.2c + 5.17)\varepsilon^2 x^{2/3} \tag{3.16}$$

Figure 4 illustrates the dependence of free surface velocity on inertia and wall movement. The figure and equation (3.16) suggests that $u(x, z=\zeta)$ increases monotonically with x and

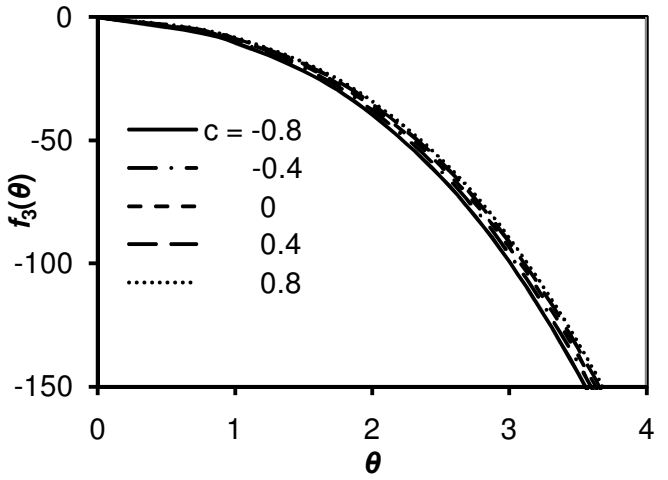

FIGURE 3. VARIATION OF THE SIMILARITY FUNCTION f_3 WITH θ FOR c ∈ [- 0.8, 0.8].

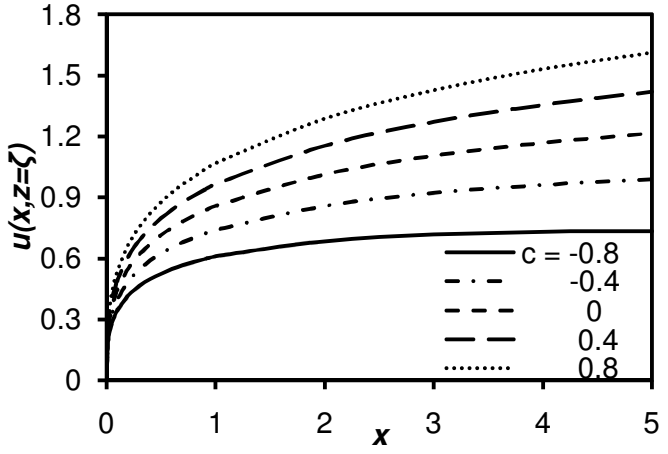

FIGURE 4. DEPENDENCE OF THE STREAMWISE VELOCITY AT THE FREE SURFACE, u(x, z = ζ), ON WALL VELOCITY FOR c ∈ [- 0.8, 0.8].

grows close to linearly with *c*.

The variation of the velocity profiles with respect to height, η, at $x = 1$, is displayed in figure 5 for different *c* values and ε = 0.1. The figure shows the gradual flattening of the velocity profile near the free surface as c decreases. The figure indicates that the asymptotic solution tends to underestimate the velocity level for any *c* value. The boundary layer height coincides with the level at which the asymptotic and inner velocity profiles begin to merge, as demonstrated in the figure.

4. THE FLOW IN THE CORE REGIONS (OUTER REGIONS INSIDE AND OUTSIDE THE CHANNEL)

The flow in the core region must be examined outside the channel ($x > 0$) and inside the channel upstream from the exit ($x < 0$). The core flows inside and outside the channel must match at the channel exit ($x = 0$). In contrast, given the boundary layer character of the inner layer (inside and outside the channel), similarity solutions can be sought separately. In particular, the presence of the singularity at the origin ($x = 0$, $z = 0$) prohibits any matching, but can be totally avoided in the

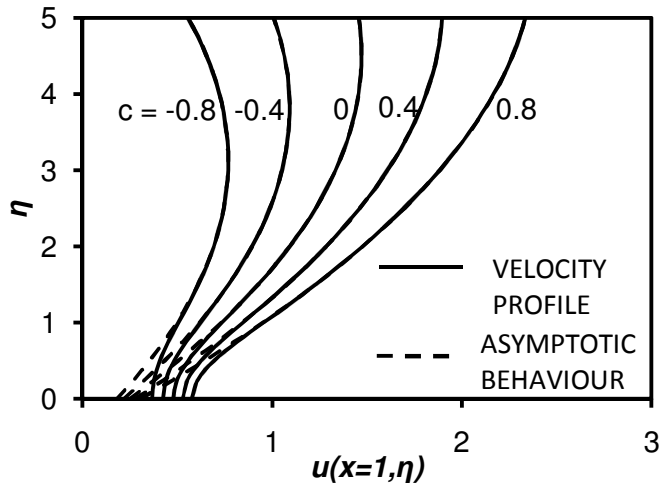

FIGURE 5. DEPENDENCE OF THE STREAMWISE VELOCITY PROFILES FOR ε = 0.2 ON HEIGHT, η, AT x = 1, FOR DIFFERENT WALL VELOCITY, c ∈ [-0.8, 0.8]. DASHED CURVES INDICATE ASYMPTOTIC BEHAVIOUR.

current formulation. In this case, the inner solution inside the channel ($x < 0$) is not required for the determination of the flow outside the channel, and therefore will not be discussed any further.

In the core region, which is far from the region near $z = 0$, the solution of equations (2.4) is sought subject to conditions (2.5) and (2.6). In this case, ψ and p are represented by the following outer expansions:

$$\psi(x,z) = \psi_0(x,z) + \varepsilon\psi_1(x,z) + \cdots \qquad (4.1a)$$

$$p(x,z) = p_0(x,z) + \varepsilon p_1(x,z) + \cdots \qquad (4.1b)$$

Here, recall that $\psi_0 = (3+c)z^2 - 2z^3$ is just the basic Poiseuille-Couette stream function given in (2.3); ψ_m (m > 0) are higher order terms that represent the deviation from the basic flow due to its interaction with the inner layer.

Since the governing equations are elliptic (in x), the deviation from the Poiseuille-Couette flow will extend also to the region $x < 0$ in the channel. Based on these assumptions, upon inserting expressions (4.1) into equations (2.4), a hierarchy of equations is obtained to each order. To leading order $p_0(x, z) = 0$. For m = 1 and 2, the matching conditions obtained in section 6, and the condition $\psi_{m>0}(x \to -\infty, z) = 0$, lead to the vanishing of the stream function and pressure everywhere. More explicitly,

$$\psi_1(x, z) = \psi_2(x, z) = p_1(x, z) = p_2(x, z) = 0 \qquad (4.2)$$

To next order, m = 3, equations (2.4) lead to

$$\psi_{0z}\psi_{3xz} - \psi_{0zz}\psi_{3x} = -p_{3x} - 12 \qquad (4.3a)$$

$$\psi_{0z}\psi_{3xx} = p_{3z} \qquad (4.3b)$$

Noting that $w_3 = -\psi_{3x}$, and using expression (2.3) the following boundary value problem in the ranges $-\infty \le x \le \infty$ and $0 \le z \le 1$ is concluded:

$$\nabla^2 w_3 + \frac{6}{(3+c)z - 3z^2} w_3 = 0 \qquad (4.4a)$$

$$\begin{aligned} &w_3(x,1) = 0 \\ &w_3(x,0) = 0 \qquad \text{for} \qquad x < 0 \\ &w_3(x, z \to 0) = -\frac{6}{3+c} \qquad \text{for} \qquad x > 0 \\ &w_3 \quad \text{bounded as } |x| \to \infty \end{aligned} \qquad (4.4b)$$

The condition $w_3(x > 0, z \to 0) = -\frac{6}{3+c}$ is obtained from matching between the inner and core region. The solution of problem (4.4) does not vanish given the non-homogeneity of the boundary conditions.

Consider now the core flow in the region inside the channel ($x < 0$). In this case, using a separation of variable argument, the solution of problem (4.4) is written as (Tillett 1968):

$$w_3(x < 0, z) = -\psi_{3x}(x < 0, z) = -\sum_{n=1}^{\infty} A_n e^{\beta_n x} V_n(z) \qquad (4.5)$$

The shape functions V_n are governed by the following eigenvalue problem:

$$V_n'' + \left(\beta_n^2 + \frac{2k}{z - kz^2}\right) V_n = 0 \qquad V_n(0) = V_n(1) = 0 \qquad (4.6)$$

where $k = \frac{3}{3+c}$ and β_n is real and positive. Note that the range of k is finite, $k \in \left(0, \frac{3}{2}\right)$. Problem (4.6) is an eigenvalue problem, which is solved subject to the additional boundary condition $V_n'(0) = 1$. For $c \ge 0$ ($k \le 1$), the problem can be solved numerically without difficulty. On the other hand, for $c < 0$ ($k > 1$), equation (4.6) admits a regular singular point at $z = 1/k$. Since k is typically not much greater than one, the solution can be obtained as a regular perturbation expansion about $k = 1$ in terms of the small parameter $\kappa = k - 1$

The stream function inside the channel is obtained by integrating expression (4.5) subject to $\psi_3(x \to -\infty, z) = 0$, leading to

$$\psi(x < 0, z) = (3+c)z^2 - 2z^3 + \varepsilon^3 \sum_{n=1}^{\infty} \frac{A_n}{\beta_n} e^{\beta_n x} V_n(z) \qquad (4.7)$$

Finally, the coefficients A_n are obtained by matching the flow at the channel exit, and will therefore be determined once the outer flow is considered for $x > 0$.

Downstream from the channel exit, the solution of problem (4.4) is given as

$$\begin{aligned} w_3(x > 0, z) = -\psi_{3x}(x > 0, z) = -\frac{6}{3+c} V_0(z) \\ + \sum_{n=1}^{\infty} A_n e^{-\beta_n x} V_n(z) \end{aligned} \qquad (4.8)$$

where $V_0(z)$ satisfies the following equation and boundary conditions:

$$V_0'' + \frac{2k}{z - kz^2} V_0 = 0, \qquad V_0(0) = 1, \qquad V_0(1) = 0 \qquad (4.9)$$

Problem (4.9) admits an analytical solution if c is different from zero (k different from one). In this case,

$$\begin{aligned} V_0(z) = 2kz(kz-1)\ln(kz|kz-1|) - 2kz + 1 + \\ z(kz-1)\left[\frac{1-2k}{1-k} - 2k\ln(k|k-1|)\right] \end{aligned} \qquad (4.10)$$

where k is defined above. For a wall with relatively large forward speed $(c \to \infty, k \to 0)$, $V_0 \to 1 - z$. For $c = 0$, the problem has two regular singular points at $z = 0$ and $z = 1$. Approximate solutions are found in the vicinity of these points. As mentioned earlier, the coefficients A_n are obtained by

matching w_3 at x = 0. In this case, equating (4.5) to (4.8) at x = 0, leads to

$$V_0(z) = \frac{3+c}{3} \sum_{n=1}^{\infty} A_n V_n(z) \tag{4.11}$$

which is a spectral representation of $V_0(z)$ in terms of the orthogonal functions $V_n(z)$. It follows from (4.11), given the orthogonality of the shape functions V_n, that

$$A_n = \frac{3\int_0^1 V_0(z) V_n(z)\, dz}{(3+c)\int_0^1 V_n^2(z)\, dz} \tag{4.12}$$

Finally, the stream function is determined upon integrating (4.8) and matching with (4.7) at x = 0 to give

$$\psi(x>0,z) = (3+c)z^2 - 2z^3 + \varepsilon^3 \left[\frac{6}{3+c} x V_0(z) + \sum_{n=1}^{\infty} \frac{A_n}{\beta_n} e^{-\beta_n x} V_n(z) \right] \tag{4.13}$$

The expression for the pressure inside and outside the channel becomes:

$$p_3(x<0,z) = -12x - \sum_{n=1}^{\infty} \frac{A_n}{\beta_n} e^{\beta_n x} \left\{ \left[2(3+c)z - 6z^2 \right] V_n' - \left[2(3+c) - 12z \right] V_n \right\} \tag{4.14}$$

$$p_3(x>0,z) = - \sum_{n=1}^{\infty} \frac{A_n}{\beta_n} e^{-\beta_n x} \left\{ \left[2(3+c)z - 6z^2 \right] V_n' - \left[2(3+c) - 12z \right] V_n \right\} \tag{4.15}$$

Incidentally, these expressions remain valid both in the inner and core layer as $\varepsilon^3 p_3(x,z)$ turns out to be equal to the composite pressure (see section 5). In other words, the pressure everywhere is readily available and is given by $p(x,z) \sim \varepsilon^3 p_3(x,z)$

The height of the free surface is found by matching the inner and core solution,

$$\zeta(x) = \varepsilon c_1(c) x^{1/3} + \varepsilon^2 \frac{c_2(c)}{2(3+c)} x^{2/3} \tag{4.16}$$

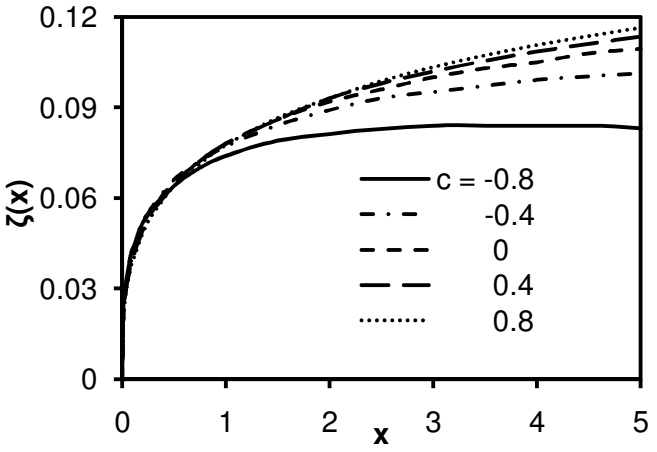

FIGURE 6. DEPENDENCE OF THE FREE SURFACE HEIGHT, ζ(X), ON WALL VELOCITY FOR c ∈ [- 0.8, 0.8].

The surface profiles are shown in figure 6 for ε = 0.1 and $c \in$ [-0.8, 0.8], which suggest a significant thickening of the film when the wall is moving backwards. The surface height also exhibits a maximum at a position $x_m = -\left[\frac{(c+3)c_1}{\varepsilon c_2} \right]^3$, which turns out to be simply proportional to the Reynolds number. Interestingly, the actual value of the maximum surface height, $\zeta_m = \zeta(x = x_m)$, is independent of the Reynolds number, and is given by $\zeta_m = -\frac{c_1^2(c+3)}{2c_2}$.

5. COMPOSITE FLOW OUTSIDE THE CHANNEL

Following Van Dyke [12], the composite expansion operator is defined by

$$C_n \equiv (E_n + H_n - E_n H_n) \tag{5.1}$$

where m and n are integers. Here, E_n is the core-expansion operator, which truncates immediately after the term of order ε^n where the expansion is expressed in terms of core variables. H_m is the corresponding inner- or outer-expansion operator.

For n = m = 3, the composite expansion for the stream function becomes,

$$C_3\psi(x,z)=\varepsilon^2 x^{2/3}\left[f_2(\theta)-\frac{6}{2(3+c)}z^2c_2\right]$$
$$+\varepsilon^3\left\{xf_3(\theta)+\psi_3(x,z)-\frac{6}{3+c}x+2\left[(3+c)z-3z^2\right]h_2(x)\right\}+O\left(\varepsilon^4\right)$$
(5.2)

Although the value of $h_2(x)$ is required if the stream function is to be evaluated to $O(\varepsilon^3)$, this accuracy is not indispensible when the flow variables are determined. This is the case, for instance, for the following expressions for the streamwise and transverse velocity components:

$$C_2u(x,z)=\varepsilon x^{1/3}f_2'(\theta)+\varepsilon^2x^{2/3}\left[f_3'(\theta)-\frac{6}{3+c}zc_2\right]+O\left(\varepsilon^3\right)$$
(5.3)

$$C_2w(x,z)=-\frac{\varepsilon^2}{3}x^{-1/3}\left[2f_2(\theta)-(\theta+c_1)f_2'(\theta)\right]+O\left(\varepsilon^3\right)$$
(5.4)

These expressions dictate how the velocity profile changes over the width of the jet up to the second order. This is also the case of the pressure, with non-zero contribution entering only to third order, namely

$$C_3p(x,z)=$$
$$-\varepsilon^3\sum_{n=1}^{\infty}\frac{A_n}{\beta_n}e^{-\beta_nx}\left\{\left[2(3+c)z-6z^2\right]V_n'-\left[2(3+c)-12z\right]V_n\right\}$$
$$+O\left(\varepsilon^4\right)$$
(5.5)

The composite flow field (velocity and pressure) for stationary plate at different x positions between the free surface and the moving wall are shown in figure 7(a-c) with ε = 0.1. The u profiles in figure 7 indicate that the flow behaves close to fully developed at the channel exit, with the transverse velocity exhibiting a singularity like $x^{-1/3}$. Further downstream, the u profile exhibits a change in concavity at a location x that is essentially independent of c. The velocity profiles are similar to the ones measured by Maki [13] for a wall jet without a free surface. The boundary layer height is also shown in the figures for each case, indicating the relatively fast growth for a backward moving wall.

The w profiles do not show any qualitative dependence on wall velocity, with w gradually diminishing with x after the jump at the channel exit. The transverse component of the flow is essentially absent except very close to the free surface. The velocity reflects the strong presence of both shear and elongation in the flow. Near the channel exit, elongation is clearly dominant at the free surface where most of the dissipation rate is concentrated. Further downstream, most of the dissipation occurs above the free surface. The pressure profile suggests overall the existence of strong and intricate pressure variation across the jet. Also, the pressure tends to decay to zero over a relatively short distance from channel exit,

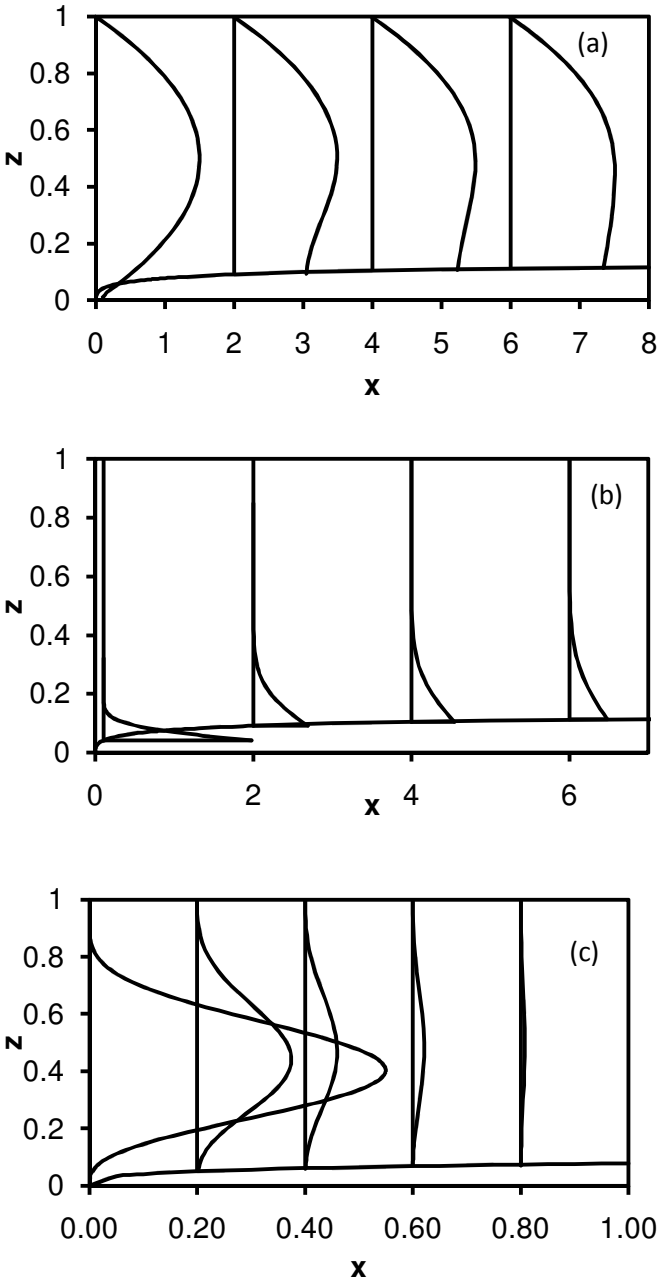

FIGURE 7. VARIATION OF STREAMWISE VELOCITY (a), TRANSVERSE VELOCITY (b) AND PRESSURE (c) PROFILES WITH POSITION FOR ε = 0.2, FOR A STATIONARY WALL (*c* = 0).

typically on the order of less than one channel width. The pressure in figure 9 exhibits a maximum located at higher z position as x increases and then decreases to zero at the upper wall.

Further insight on the role of elongation is gained by examining the change in excess normal stress with position, namely, $C_2 u_{xx}(x,z)$, which is readily available from (5.3). Figure 8 illustrates the influence of wall movement on elongational flow, where $C_2 u_{xx}(x, z = 0.5)$ is plotted for $c \in [-0.8, 0.8]$ and ε = 0.1. The figure shows the influence of the singularity in stress, felt at a location above the free surface. This is in agreement with stress gradient profiles reported by Lee *et al*. (2002) for planar injection flow. The stress gradient is anti-symmetric with respect to the origin, with negative or positive slope depending on whether the wall is moving backward or forward, respectively. For strongly backward moving wall, illustrated here by the c = - 0.8 profiles, the stress gradient is relatively mild, negative inside the channel and positive outside. When c decreases toward zero, the overall stress gradient decreases, but reflects a stronger singularity at the exit, with a stagnation point right upstream from the exit.

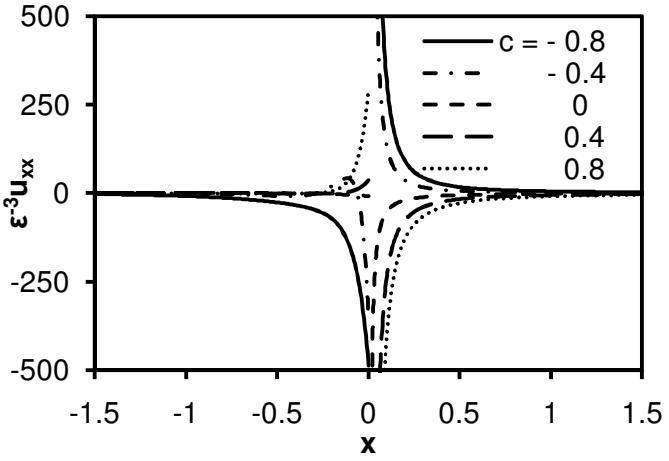

FIGURE 8. INFLUENCE OF WALL VELOCITY ON THE VARIATION OF NORMAL STRESS GRADIENT WITH POSITION AT z = 0.5 FOR ε = 0.1.

Thus, although relatively high stress level is achieved when the wall is stationary, most of the stress accumulated is relaxed in the exit region. There is a change in sign as c increases further and becomes positive, and the singularity weakens again.

8. CONCLUDING REMARKS

The two-dimensional wall jet flow of a Newtonian fluid emerging from a channel and adhering to a moving wall is examined in this study. The wall may move backward ($c < 0$) or forward ($c > 0$), opposing or in contestation with the pressure gradient applied far upstream in the channel. Inertia is assumed to be large enough, allowing asymptotic development in terms of the inverse Reynolds number. In this case, the equations of motion are reduced by expanding the flow field about the basic Poiseuille-Couette flow. Similarly to the flow with fine to moderate constriction (Smith [14-16]), the core flow is essentially inviscid rotational. A classical boundary layer analysis is applied to find the flows adjacent to the free surface and the moving wall, where a boundary layer forms for moderate distances downstream from the channel exit. The influence of this boundary layer is investigated by the aid of the method of matched asymptotic expansions. The roles of inertia of the incoming jet and wall velocity are emphasized.

The boundary layer structures near the free surface and the moving wall were examined in detail. The viscous relaxation length for diffusion of stress singularity was found, as expected, to increase with inertia, with a corresponding thinning in the boundary layer. On the other hand, the relaxation length is found to be uninfluenced by wall velocity for a forward moving wall. In contrast, the diffusion length decreases rapidly with the velocity of a backward moving wall. Although the flow field and jet profiles seem to be qualitatively insensitive to wall movement, the pressure exhibits an unexpectedly varied response. Instead of the monotonically decreasing pressure profile typically predicted for a jet (Tillett 1968), the pressure displays a minimum near the free surface, which is gradually replaced by a strong maximum near the moving wall. The upstream distance from the channel exit where fully developed conditions are reached is essentially independent of c for $c > 0$, but decreases significantly to reach approximately five times the width of the channel when the velocity of the backward moving wall is twice the mean Poiseuille velocity (c = - 1).

Finally, the significance of the current study and the advantages of the proposed formulation cannot be overstated. In typical jet flow calculations in the literature, fully developed conditions are assumed at inception. The present work provides the correct conditions near exit, which are required to determine the jet structure further downstream. The current formulation also allows for the determination of the steady state flow and free surface profiles analytically. The availability of the steady state in analytical form constitutes a significant advantage for a linear stability analysis on the jet (Soederberg [17]), and, as often is the case, when the steady state is taken as the initial condition for a transient analysis. The accuracy of initial conditions is crucial, for instance, for a thin jet given the hyperbolicity of the problem (Khayat & Kim [18]).

REFERENCES

[1] Watson, E., 1964, "The Spread of a Liquid Jet Over a Horizontal Plane,'' J. Fluid Mech., **20**, pp. 481.

[2] Ruschak, K. J., 1985, "Coating Flows,'' Ann. Rev. Fluid Mech., **17**, pp. 65-89.

[3] Weinstein, S. J. and Ruschak, K. J., 2004, "Coating Flows,'' Ann. Rev. Fluid Mech., **36**, pp. 29.

[4] Carvalho, M. S. and Kheshgi, H. S., 2000, "Low-Flow Limit in Slot Coating: Theory and Experiments,'' AIChE J., **46**(10), pp. 1907.

[5] Pasquali, M. and Scriven, L.E., 2002, "Free Surface Flows of Polymer Solutions with Models Based on the Conformation Tensor,'' J. Non-Newtonian Fluid Mech., **108**, pp. 363.

[6] Lee, A. G., Shaqfeh, E. S. G. and Khomami, B, 2002, "A Study of Viscoelastic Free Surface Flows by the Finite Element Method: Hele-Shaw and Slot Coating Flows,'' J. Non-Newtonian Fluid Mech., **108**, pp. 327.

[7] Romero, O. J., Scriven, L.E. and Carvalho, M. S., 2006, "Slot Coating of Mildly Viscoelastic Liquids,'' J. Non-Newtonian Fluid Mech., **138**, pp. 63-75.

[8] Ross, A. B., Wilson, S. K. and Duffy, B. R., 1999, "Blade Coating of a Power-Law Fluid,'' *Phys. Fluids* ,**12**(5), pp. 958.

[9] Ro, J. S. and Homsy, G. M., 1995, "Viscoelastic Free Surface Flows: Thin Film Hydrodynamics of Hele-Shaw and Dip Coating Flows,'' J. Non-Newtonian Fluid Mech., **57**, pp. 203.

[10] Tillett, J. P. K., 1968, "On the Laminar Flow in a Free Jet of Liquid at High Reynolds Numbers,'' J. Fluid Mech., **32**, pp. 273.

[11] Goldstein, S**.,** 1960, *Lectures in Fluid Mechanics,* (Interscience, New York).

[12] Van Dyke, M. D., 1964, *Perturbation Methods in Fluid Mechanics*, (Academic Press, New York).

[13] Maki, H., 1983, "Experimental studies on the combined flow filed formed by a moving wall and a wall jet running parallel to it,'' Bullt. Japan Soc. Mech Eng. **26**, pp. 2100.

[14] Smith, F.T., 1976, "Flow through Constricted or Dilated Pipes and Channels: Part 1,'' Q.Jl Mech. appl. Math., **29**, pp. 343.

[15] Smith, F.T., 1976, "Flow through Constricted or Dilated Pipes and Channels: Part 2,'' Q.Jl Mech. appl. Math., **29**, pp. 365.

[16] Smith, F.T., 1979, "The Separating Flow through a Severely Constricted Symmetric Tube,'' J. Fluid Mech., **90**, pp. 725.

[17] Soederberg, L. D., 2003, "Absolute and Convective Instability of a Relaxational Plane Liquid Jet,'' J. Fluid Mech., **493**, pp. 89.

[18] Khayat, R. E. and Kim, K., 2002, "Influence of Initial Conditions on Transient Two-Dimensional Thin-Film Flow,'' Phys. Fluids, **14**, pp. 4448.